Journal of Alloys and Compounds 556 (2013) 26–31

Contents lists available at SciVerse ScienceDirect

Journal of Alloys and Compounds

journal homepage: www.elsevier.com/locate/jalcom

Enhanced ductility of the ZA85 magnesium alloy fabricated by equal-channel angular pressing

Che-Yi Lin [a], Hui-Yum Bor [b], Chuen-Guang Chao [a,*], Tzeng-Feng Liu [a]

[a] Department of Materials Science and Engineering, National Chiao Tung University, 1001 Ta Hsueh Road, Hsinchu City 30010, Taiwan
[b] Materials & Electro-Optics Research Division, Chung-Shan Institute of Science & Technology, 481 Sec. Chia An, Zhongzheng Road, Longtan Shiang, Taoyuan County 325, Taiwan

ARTICLE INFO

Article history:
Received 2 November 2012
Received in revised form 13 December 2012
Accepted 18 December 2012
Available online 26 December 2012

Keywords:
ZA85 magnesium alloy
Equal-channel angular pressing
Enhanced ductility
Thermal stability

ABSTRACT

Equal-channel angular pressing (ECAP) was applied to the as-cast Mg–8 wt.%Zn–5 wt.%Al (ZA85) alloy to produce a fine-grained structure with fine and uniformly distributed $Mg_{32}(Al, Zn)_{49}$ (τ-phase) particles. Experiments showed that the ZA85 alloy had an initial grain size of ~150 μm after casting and was significantly reduced to 4 μm after six ECAP passes at 180 °C. After annealing at 300 °C for 1 h, the average grain size merely increased to 7.1 μm. This thermal stability of the fine-grained structure at temperatures at or below 325 °C is attributed to the presence of the fine and well distributed τ-phase. It was demonstrated that ECAP processing greatly enhances ductility of the experimental alloy. By testing over a range of temperatures and strain rates, a maximum elongation to failure of 400% was obtained in the ECAP ZA85 alloy tested at 300 °C (0.53 T_m) with the initial strain rate of 1.0×10^{-4} s^{-1}. The dominant deformation mechanism for the specimens tested at 300 and 350 °C with the initial strain rates ranging from 1.0×10^{-4} s^{-1} to 1.0×10^{-3} s^{-1} is GBS controlled by grain boundary diffusion. At the higher testing temperature of 400 °C, the deformation mechanism for the experimental alloy is dislocation creep.

© 2012 Elsevier B.V. All rights reserved.

1. Introduction

Combinations of light weight and high strength magnesium (Mg) alloys represent ideal materials for a wide range of applications in the automobile and aerospace industries [1,2]. However, owing to the closed-packed hexagonal (HCP) crystal structure, Mg alloys have a poor plasticity at room temperature (RT) and a limited forming and machining ability. Consequently, their potential applications are limited [3,4]. Superplastic forming (SPF), defined as elongations of at least 400% and strain rate sensitivity close to 0.5, is an effective method to fabricate hard-to-form materials into complex shapes [5,6]. For SPF to be used in industry, the development of high strain-rate superplasticity (HSRSP), defined as superplasticity occurring at strain rates at or above 1.0×10^{-2} s^{-1} [7], is needed, especially for Mg alloys with poor formability. Figueiredo and Langdon [8] proposed two strategies for achieving HSRSP in Mg alloys processed by equal-channel angular pressing (ECAP): (i) by pressing the alloys through a reduced number of passes in order to increase the thermal stability of the microstructure; and (ii) by increasing the processing temperature to permit the occurrence of superplastic flow at higher testing temperatures. Another desirable property for developing superplasticity in a material is low temperature superplasticity (LTSP), defined as superplasticity occurring at temperatures at or below 0.55 T_m, where T_m is the alloy melting temperature [7]. The presence of LTSP is an attractive property in Mg alloys because of their susceptibility to surface oxidation when formed at elevated temperatures and their low formability at temperatures close to RT.

Many previous experiments established that superplasticity requires a small polycrystalline grain size (typically less than 10 μm [9]) and these small grains are generally achieved through the application of severe plastic deformation (SPD). ECAP is one of the most popular SPD methods and has proved to be effective in refining grains in various Mg alloys, resulting in improved ductility, strength, and superplasticity [10–20]. Matsubara et al. [11] reported that the Mg–9% Al alloy processed by a combination of extrusion and ECAP exhibited a maximum elongation of 840% at 200 °C with a strain rate of 3.3×10^{-4} s^{-1}. Figueiredo and Langdon [12] reported that an ECAP ZK60 alloy showed a maximum elongation of 3050% at 200 °C with a strain rate of 1.0×10^{-4} s^{-1}. Chuvil'deev et al. [13] found that the ECAP AZ91 alloy possessed 570% in elongation at 300 °C with a strain rate of 3.0×10^{-3} s^{-1} and the ECAP ZK60 alloy exhibited 810% in elongation at 260 °C with a strain rate of 3.0×10^{-3} s^{-1}. Liu et al. [16] reported that the as-rolled LZ82 alloy exhibited superplasticity with a maximum elongation of 430% at 225 °C and of 120% even at 150 °C. Miyahara et al. [17] found that the ECAP AZ61 possessed 1320% at 200 °C with a strain rate of 3.3×10^{-4} s^{-1}. Kawasaki and Langdon [18] also provided a very detailed tabulation of all papers reporting superplasticity in metals processed by ECAP.

* Corresponding author. Tel.: +886 3 5731809; fax: +886 3 5724727.
E-mail address: cgchao@mail.nctu.edu.tw (C.-G. Chao).

0925-8388/$ - see front matter © 2012 Elsevier B.V. All rights reserved.
http://dx.doi.org/10.1016/j.jallcom.2012.12.090

In the present study, the ZA85 alloy was chosen as the experimental alloy because Mg–Zn–Al (ZA) alloys have been developed as new high-strength Mg alloys for elevated-temperature applications [19,21]. The poor high-temperature properties of commercial Mg–Al–Zn (AZ) alloys are attributed to the presence of intermetallic $Mg_{17}Al_{12}$ (β-phase), which mainly precipitates along grain boundaries and exhibits a low decomposition temperature. Thus, grain boundary sliding (GBS) occurs even at temperatures below 150 °C [22,23]. It has been reported that a ternary addition of a large amount of zinc to binary Mg–Al alloys, with a Zn:Al composition of approximately 2:1, can completely suppress the formation of the β-phase [19,21,24]. The main precipitate of the ZA alloy is the τ-phase that has a higher melting point and decomposition temperature than the β-phase [25], leading to better properties at elevated temperatures than commercial AZ alloys. In this study, ECAP was used to refine grains and precipitates, and to eliminate defects for enhancing ductility in the ZA85 alloy. It was found that the ECAP ZA85 alloy exhibits LTSP. The mechanism and activation energy of deformation of the experimental alloy were also investigated.

2. Experimental details

An alloy with a composition of Mg–8 wt.%Zn–5 wt.%Al (ZA85) was prepared. Pure Mg, Al, and Zn (>99.9%) were melted at 750 °C with SF_6 as the protective atmosphere. Steel molds with cavity dimensions of 300 mm × 70 mm × 60 mm were used for casting the alloy. The as-cast alloy in the molten state was air cooled. The chemical composition of the alloy was 8.34 wt.%Zn, 4.74 wt.%Al with the balance Mg.

For the ECAP process, the dimensions of the specimens are 17 mm × 17 mm × 60 mm, and an ECAP die with 120° angle was used. Boron nitride was used as the lubricant during ECAP. An ECAE temperature of 180 °C was used because higher ECAP temperatures would have led to grain growth [19]. The ECAP die was preheated to 180 °C and maintained for 15 min before inserting a lubricated ECAP specimen into the entrance channel. The specimen was held inside the ECAP die for 5 min before pressing. The ECAP process was conducted via Route B_C in which the specimen was rotated through 90° in the same direction after each pass with a pressing speed of 2 mm/min.

Following the ECAP process, some samples were sliced perpendicular to the longitudinal axes to a 3 mm thickness. These small disks were sealed in glass tubes under vacuum and annealed for 1 h at selected temperatures ranging from 200 to 400 °C. These static annealing experiments were used to observe the thermal stability of the microstructure.

Microstructures of the as-cast and ECAP materials were examined using standard metallographic procedures. The polished surfaces were etched with 3 mL acetic acid solution, 5 mL deionized water, 35 mL ethanol, and 1 g picric acid. The microstructures were observed by optical microscopy and scanning electron microscopy (SEM). The average grain size was determined with Image Pro software (IpWin32).

The tensile tests were conducted over temperatures ranging from 250 to 400 °C with the initial strain rates ranging from 1.0×10^{-2} to 1.0×10^{-4} s^{-1}, using a testing machine operating at a constant cross-head displacement rate. The tensile specimens were longitudinally cut from the samples after ECAP by wire-electrode cutting and were made with a gauge section of 6 mm × 3 mm × 2 mm. The specimens were heated to the selected temperatures and then held for 10 min prior to the tensile tests. All tensile specimens were pulled to failure to obtain information on the total elongations.

3. Experimental results and discussion

3.1. Microstructures in the ZA85 alloy

Fig. 1 shows the optical micrograph of the as-cast ZA85 alloy. The initial grain size of ~150 μm was obtained with an equiaxed grain structure. The coarse precipitates, identified as the τ-phase by X-ray diffraction (the same as in prior literature [24–26]), were distributed along the grain boundaries. Furthermore, defects such as blow holes and shrinkage voids were clearly observed in the as-cast specimens. These defects resulted from the air trapped in the melting alloy during casting and from the difference between the cooling rates in the inner and outer regions of the ingot. Fig. 2 shows the microstructure of the ECAP ZA85 alloy. After six

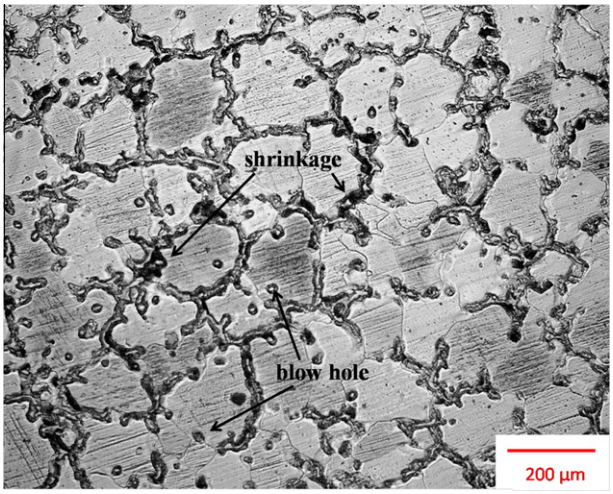

Fig. 1. Optical micrograph of the as-cast ZA85 alloy.

ECAP passes at 180 °C, the average grain size was significantly reduced to 4 μm, as shown in Fig. 2a. The mechanism of grain refinement for Mg alloys by ECAP was dynamic recrystallization (DRX) [19,27,28]. DRX led to the production of equiaxed grains with a high fraction of high-angle grain boundaries. In addition, defects such as blow holes and shrinkage voids were totally eliminated by ECAP. The precipitate size was also refined during the ECAP process; it was greatly reduced to an average of 1 μm with uniform distribution after six ECAE passes at 180 °C, as shown in Fig. 2b.

3.2. Thermal stability of the fine-grained structure

The ECAP samples were subjected to a static annealing treatment for 1 h at selected temperatures ranging from 200 to 400 °C to investigate the thermal stability of the fine-grained structure. The results are shown in Figs. 3 and 4 and it is apparent that there was reasonable grain stability up to 325 °C; however, at higher temperatures, there was grain growth yielding grain sizes of ~13.7, ~21.0, and ~36.5 μm after annealing at 350, 375, and 400 °C, respectively. The SEM micrographs (Fig. 4) show the microstructures of the ECAP samples after annealing at 300, 350, and 400 °C. After annealing at 300 °C for 1 h, the average grain size merely increased to 7.1 μm, which is still desirable for superplastic deformation. This thermal stability of the fine-grained structure at the temperatures at or below 325 °C is attributed to the presence of the fine and well-distributed τ-phase, which inhibits grain-boundary migration. With the annealing temperature higher than 350 °C, the average grain size increased to above 10 μm and the fine precipitates were gradually dissolved into the matrix. Fig. 4c shows that after annealing for 1 h at 400 °C, the fine precipitates were hardly observed in the microstructure and the average grain size increased to 36.5 μm.

3.3. Tensile testing of the ZA85 alloy

Fig. 5 shows the stress versus elongation to failure for samples processed by six ECAP passes at 180 °C and then pulled to failure in tension at temperatures ranging from 250 to 400 °C with the initial strain rates from 1.0×10^{-2} to 1.0×10^{-4} s^{-1}. The outer appearance of the testing specimens is illustrated in Fig. 6, where the upper specimen is untested and the other specimens were pulled to failure under the selected conditions. A maximum elongation of 400% was achieved at 300 °C with the initial strain rate of 1.0×10^{-4} s^{-1}. The necking phenomenon observed in the speci-

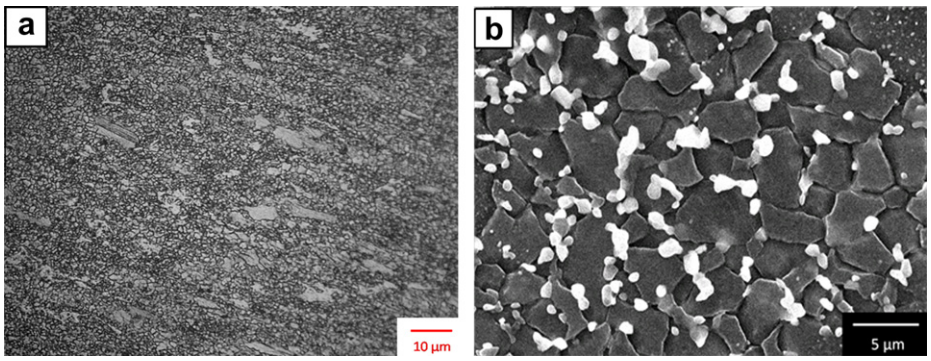

Fig. 2. (a) Optical micrograph and (b) SEM micrograph of the ZA85 alloy fabricated by ECAP with six passes at 180 °C.

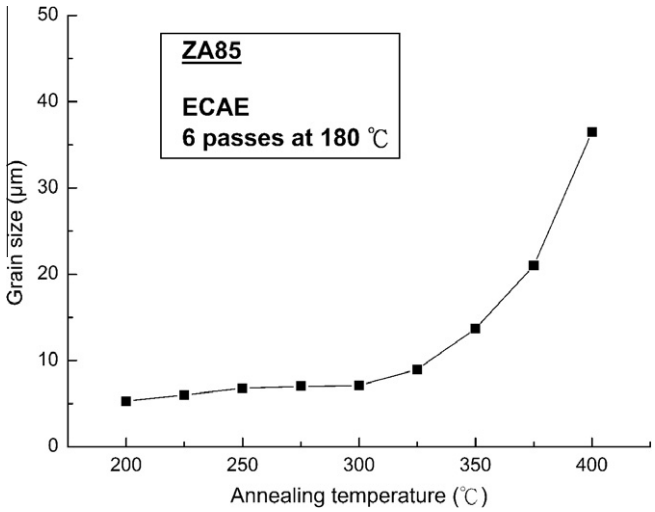

Fig. 3. Grain size versus annealing temperature after static annealing of the material processed by ECAP with six passes at 180 °C.

mens tested at 300 and 350 °C with initial strain rates of $1.0 \times 10^{-3}\ s^{-1}$ and $1.0 \times 10^{-4}\ s^{-1}$ is very similar to that previously reported for Mg-based alloys [11,29]. It is worth mentioning that the flow stress was relatively uniform without apparent strain hardening when testing at higher temperatures with lower initial strain rates. This phenomenon is ascribed to the occurrence of strain softening under higher temperatures and lower initial strain rates, which compensated for the effect of strain hardening.

Fig. 7 shows the elongation to failure versus the initial strain rate for the ECAP samples. The inspection of Fig. 7 provides four significant trends. First, the maximum elongation achieved at each temperature tends to increase with temperature up to 300 °C, but decreases at higher temperatures of 350 and 400 °C. This is attributed to the rapid grain growth occurring above 350 °C, as demonstrated in Figs. 3 and 4. Second, the elongations generally increase with decreasing initial strain rates, except at 400 °C where the peak elongation is achieved at $1.0 \times 10^{-3}\ s^{-1}$, and the elongation decreases when the initial strain rate is reduced to $1.0 \times 10^{-4}\ s^{-1}$. Third, for testing temperatures of 350 and 400 °C, higher elongations are achieved at the initial strain rate of $1.0 \times 10^{-2}\ s^{-1}$ with a testing temperature of 400 °C, but the situation reverses for ini-

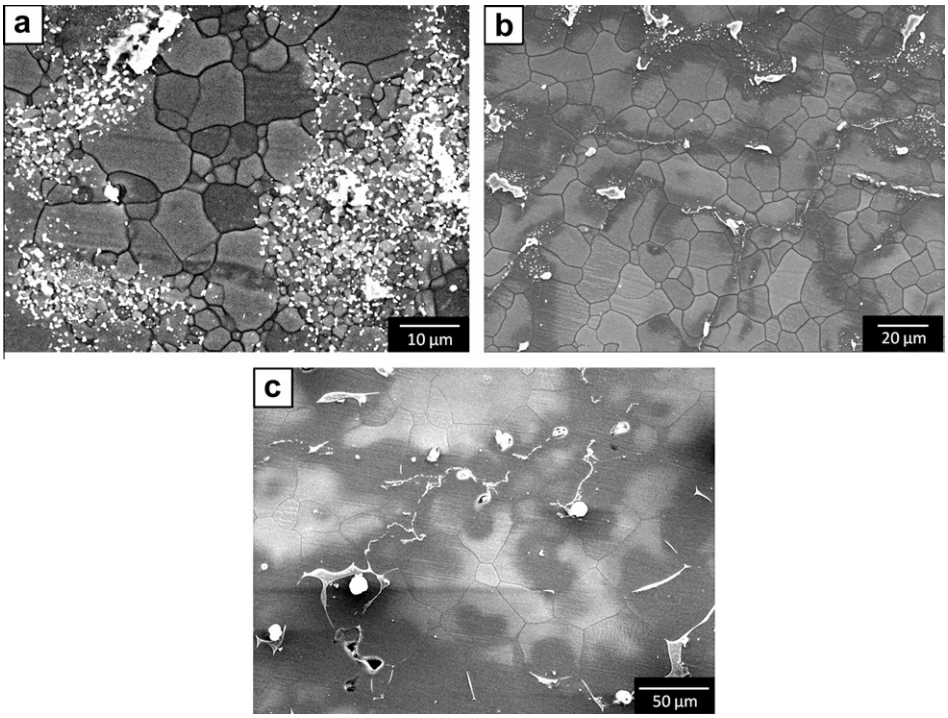

Fig. 4. SEM micrographs of the ECAP ZA85 alloy after static annealing for 1 h at (a) 300, (b) 350, and (c) 400 °C.

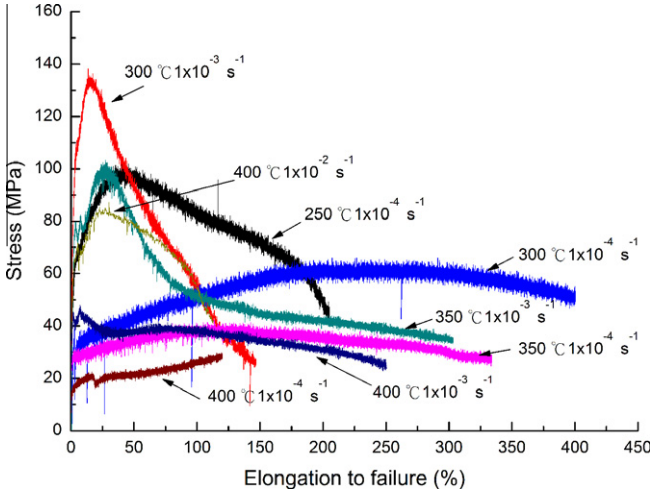

Fig. 5. Stress versus elongation to failure for the ECAP ZA85 alloy at the testing temperatures ranging from 250–400 °C with the initial strain rates from 1.0×10^{-2} to 1.0×10^{-4} s^{-1}.

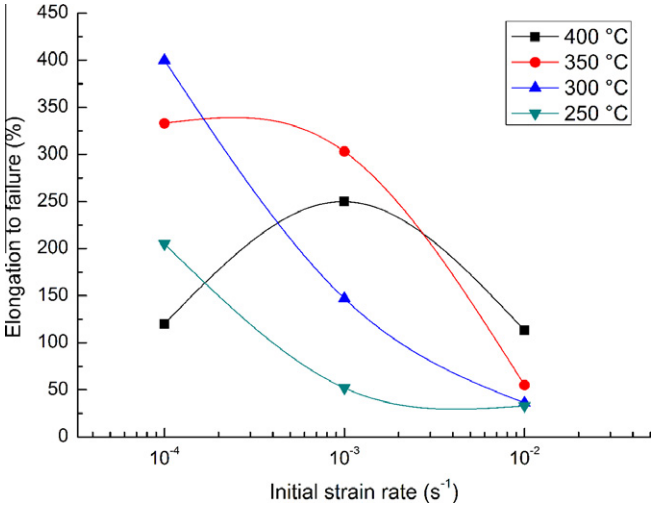

Fig. 7. Elongation to failure versus initial strain rate over a range of temperatures for the ECAP ZA85 alloy.

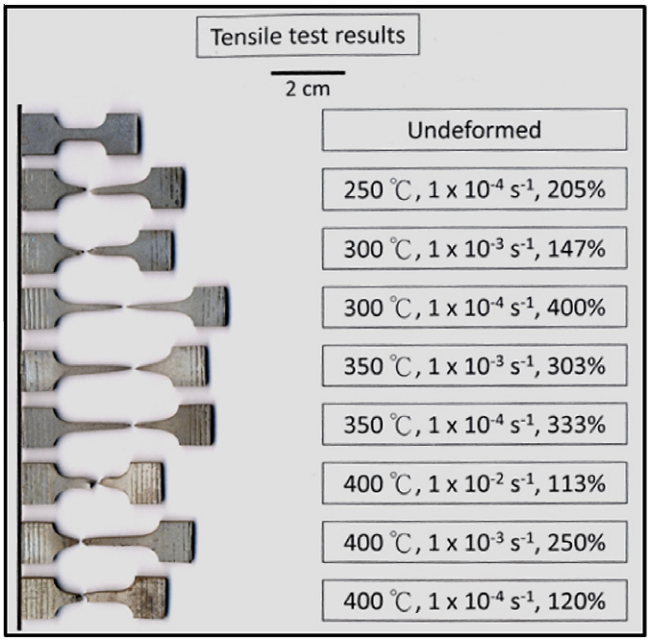

Fig. 6. Appearance of the specimens processed by ECAP with six passes at 180 °C and subsequently tested in tensile to failure under the selected conditions.

tial strain rates at and below 1.0×10^{-3} s^{-1}. The higher elongation achieved at 400 °C with the higher initial strain rate of 1.0×10^{-2} s^{-1} is ascribed to the short testing time that limits grain growth within the specimens during tensile testing. On the other hand, the lower strain rate allows grains to have sufficient time to grow, leading to a reduction in the elongations when tested at 400 °C in comparison with the tests conducted at 350 °C. Fourth, the melting temperature of the ZA85 alloy is about 570 °C [30]. At 300 °C, which corresponds to 0.53 T_m, an elongation to failure of 400% is obtained with initial strain rate of 1.0×10^{-4} s^{-1}. This result clearly demonstrates the occurrence of LTSP in the experimental alloy. The presence of LTSP is an attractive property in Mg alloys because of their susceptibility to surface oxidation when formed at elevated temperatures and their low formability at temperatures close to RT. Furthermore, even at the lower temperature of 250 °C, which corresponds to 0.44 T_m, elongation to failure of 205% is achieved with the initial strain rate of 1.0×10^{-4} s^{-1}. At a testing temperature of 400 °C, an elongation to failure of 113% is achieved with the initial strain rate of 1.0×10^{-2} s^{-1}. Therefore, after the ECAP process at 180 °C with six passes, the ductility of the ZA85 alloy is greatly enhanced.

Fig. 8 shows the flow stress versus the initial strain rate for the experimental alloy under the selected testing conditions. The strain rate sensitivity exponent (m value), which is obtained from the slopes of the fitted lines, is an important parameter during superplastic deformation. Superplastic deformation is an integrated process that combines GBS, dislocation movement, and diffusion in intracrystalline. The m value represents the proportion of GBS, and it is well known that high strain rate sensitivity (typically m close to 0.5) is a characteristic of superplastic metals and alloys [6,31]. The stress exponent (n value), which is reciprocal of the m value, was calculated to determine deformation mechanism of the experimental alloy. The results show that the m values of 0.55 and 0.45 corresponding to $n = 1.81$ and 2.22 were obtained with the initial strain rate ranging from 1.0×10^{-4} s^{-1} to 1.0×10^{-3} s^{-1} at 300 and 350 °C, respectively. It has been reported that the n value of the GBS and the dislocation creep mechanisms are 2

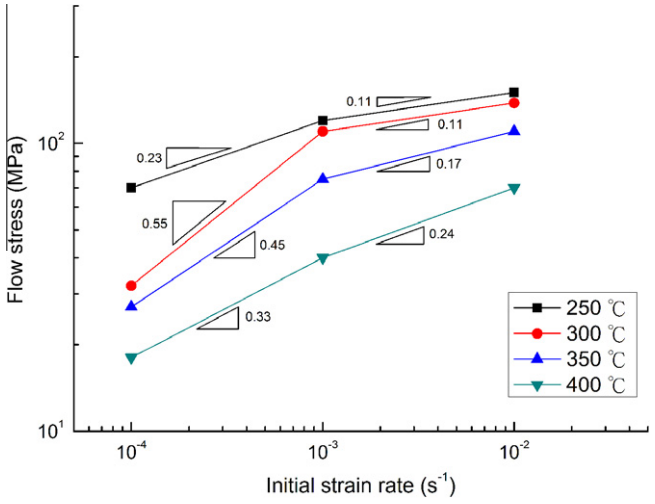

Fig. 8. Flow stress versus initial strain rate over a range of temperatures for the ECAP ZA85 alloy.

and 3, respectively [31,32]. Therefore, the deformation mechanism for the specimens tested at 300 and 350 °C with the initial strain rate ranging from $1.0 \times 10^{-4}\ s^{-1}$ to $1.0 \times 10^{-3}\ s^{-1}$ is GBS. At 400 °C, the n value is 3.03 ($m = 0.33$), which means that the deformation mechanism is dislocation creep.

It has been reported that GBS is accommodated by slip controlled by diffusion [33]. To further understand the mechanism for the specimens tested at 300 and 350 °C with the initial strain rate ranging from $1.0 \times 10^{-4}\ s^{-1}$ to $1.0 \times 10^{-3}\ s^{-1}$ during the deformation process, the activation energy for the deformation was calculated under constant strain rate using the following formula [34]:

$$Q = nR\frac{\partial(\ln \sigma)}{\partial(1/T)}$$

where Q is the apparent activation energy, n is the stress exponent, R is the gas constant ($R = 8.31$ J/(K mol)), σ is the true stress, and T is the absolute temperature. It has been reported that the activation energy in Mg alloys for grain boundary diffusion and for lattice diffusion are 92 and 135 kJ mol^{-1}, respectively [35,36]. According to the relationship of ln σ versus $1/T$ at different strain rates during the deformation, the activation energy Q in the ECAP ZA85 alloy tested with the initial strain rate of $1.0 \times 10^{-4}\ s^{-1}$ was calculated to be 88.5 kJ mol^{-1}, which is very close to the value for grain boundary diffusion. When increasing the initial strain rates to $1.0 \times 10^{-3}\ s^{-1}$ and $1.0 \times 10^{-2}\ s^{-1}$, activation energies Q of 105 and 118 kJ mol^{-1} were estimated, respectively, which are higher than those for grain boundary diffusion but lower than those for lattice diffusion. Therefore, the dominant deformation mechanism of the ECAP ZA85 alloy tested at temperatures ranging from 300 to 350 °C is GBS controlled by grain boundary diffusion.

3.4. Fracture surface of the ECAP sample after tensile testing

Fig. 9 shows the tensile fracture surface of the ECAP specimens tested with the initial strain rate of $1.0 \times 10^{-3}\ s^{-1}$ at 250, 300, 350, and 400 °C. In general, the failure of Mg alloys is brittle through cleavages at RT because of their HCP structure. Fig. 9a shows that the fracture surface for the ECAP sample tested at 250 °C with the initial strain rate of $1.0 \times 10^{-3}\ s^{-1}$ showed mainly cleavages. Fig. 9b shows that the fracture surface consisted of some dimples and cleavages when tested at 300 °C with the initial strain rate of $1.0 \times 10^{-3}\ s^{-1}$. This means that the deformation of the experimental alloy gradually transformed from brittle to ductile through thermal activation. Fig. 9c shows that the fracture surface totally changed to dimples when tested at 350 °C with the initial strain rate of $1.0 \times 10^{-3}\ s^{-1}$. However, when increasing the tensile testing temperature to 400 °C, the fracture surface consisted of some dimples and cleavages, as shown in Fig. 9d. This is attributed to the obvious grain growth effect at 400 °C, which decreased the elongation to failure of the sample, as can be seen in Fig. 7. Close inspection shows that the fraction of dimples in Fig. 9b is less than that in Fig. 9d. This matches the value of the elongation to failure in the materials shown in Fig. 7 with the value of the elongation that increases with the increasing fraction of dimples.

4. Conclusions

1. By applying the ECAP process with six passes at 180 °C to the as-cast ZA85 alloy, the average grain size was greatly reduced from ~150 μm to 4 μm and the precipitate size was also refined to an average of 1 μm with uniform distribution.
2. After annealing at 300 °C for 1 h, the average grain size only increased to 7.1 μm. This thermal stability of the fine-grained structure at temperatures at or below 325 °C is attributed to the presence of the fine and well distributed τ-phase.
3. The ductility of the experimental alloy is greatly enhanced by the ECAP process. A maximum elongation to failure of 400% was obtained for the ECAP ZA85 alloy tested at 300 °C with the initial strain rate of $1.0 \times 10^{-4}\ s^{-1}$.
4. In the ECAP ZA85 alloy, the dominant deformation mechanism for the specimens tested at 300 and 350 °C with the initial strain rates ranging from $1.0 \times 10^{-4}\ s^{-1}$ to $1.0 \times 10^{-3}\ s^{-1}$ is

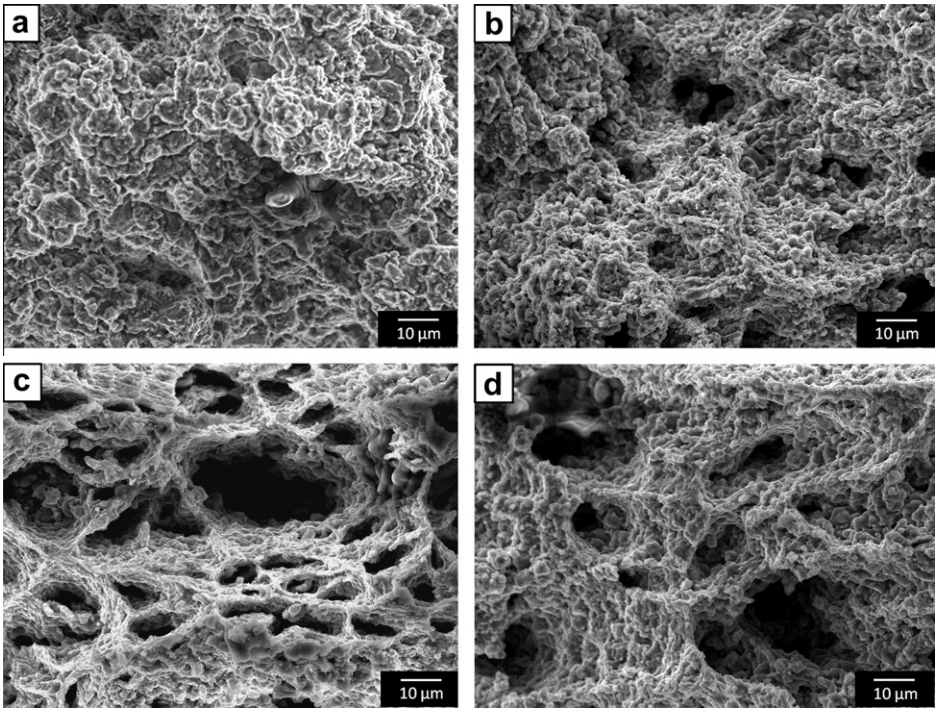

Fig. 9. Tensile fracture surface of the ECAP specimens tested with the initial strain rate of $1.0 \times 10^{-3}\ s^{-1}$ at (a) 250, (b) 300, (c) 350, and (d) 400 °C, respectively.

GBS controlled by grain boundary diffusion. At the higher testing temperature of 400 °C, the deformation mechanism for the experimental alloy is dislocation creep.

Acknowledgments

The authors are pleased to acknowledge the financial support of this research by the National Science Council, Republic of China under Grant NSC 98-2622-E-009-187-CC3.

References

[1] M. Bamberger, G. Dehm, Annual Review of Materials Research 38 (2008) 505.
[2] K. Liu, J. Meng, Journal of Alloys and Compounds 509 (2011) 3299.
[3] W.J. Kim, S.W. Chungl, C.S. Chung, D. KUM, Acta Materialia 49 (2001) 3337.
[4] L. Wu, Q. Ma, C. Zhang, Rare Metal Materials and Engineering 37 (2008) 54.
[5] R. Kaibyshev, T. Sakai, F. Musin, I. Nikulin, H. Miura, Scripta Materialia 45 (2001) 1373.
[6] T.G. Langdon, Journal of Materials Science 44 (2009) 5998.
[7] Glossary of Terms Used in Metallic Superplastic Materials, Japanese Industrial Standard, JIS H7007, 1995.
[8] R.B. Figueiredo, T.G. Langdon, Scripta Materialia 61 (2009) 84.
[9] T.G. Langdon, Metallurgical Transactions 13A (1982) 689.
[10] V.M. Segal, Materials Science and Engineering A 197 (1995) 157.
[11] K. Matsubara, Y. Miyahara, Z. Horita, T.G. Langdon, Acta Materialia 51 (2003) 3073.
[12] R.B. Figueiredo, T.G. Langdon, Advanced Engineering Materials 10 (2008) 37.
[13] V.N. Chuvil'deev, T.G. Nieh, M.Yu. Gryaznov, A.N. Sysoev, V.I. Kopylov, Scripta Materialia 50 (2004) 861.
[14] G. Ben Hamu, D. Eliezer, L. Wagner, Journal of Alloys and Compounds 468 (2009) 222.
[15] B. Chen, D.L. Lin, L. Jin, X.Q. Zeng, C. Lu, Materials Science and Engineering A 483–484 (2008) 113.
[16] X. Liu, R. Wu, Z. Niu, J. Zhang, M. Zhang, Journal of Alloys and Compounds 541 (2012) 372.
[17] Y. Miyahara, Z. Horita, T.G. Langdon, Materials Science and Engineering A 420 (2006) 240.
[18] M. Kawasaki, T.G. Langdon, Journal of Materials Science 42 (2007) 1782.
[19] C.Y. Lin, H.J. Tsai, C.G. Chao, T.F. Liu, Journal of Alloys and Compounds 530 (2012) 48.
[20] R.B. Figueiredo, T.G. Langdon, Journal of Materials Science 45 (2010) 4827.
[21] M. Vogel, O. Kraft, E. Arzt, Scripta Materialia 48 (2003) 985.
[22] A. Srinivasan, U.T.S. Pillai, B.C. Pai, Metallurgical and Materials Transactions 36 A (2005) 2235.
[23] B.H. Kim, S.W. Lee, Y.H. Park, I.M. Park, Journal of Alloys and Compounds 493 (2010) 502.
[24] Z. Zhang, A. Couture, A. Luo, Scripta Materialia 39 (1998) 45.
[25] J. Zhang, Z.X. Guo, F. Pan, Z. Li, X. Luo, Materials Science and Engineering A 456 (2007) 43.
[26] N. Balasubramani, A. Srinivasan, U.T.S. Pillai, K. Raghukandan, B.C. Pai, Journal of Alloys and Compounds 455 (2008) 168.
[27] M. Janeček, M. Popov, M.G. Krieger, R.J. Hellmig, Y. Estrin, Materials Science and Engineering A 462 (2007) 116.
[28] C.W. Su, L. Lu, M.O. Lai, Materials Science and Engineering A 434 (2006) 227.
[29] H.K. Lin, J.C. Huang, T.G. Langdon, Materials Science and Engineering A 402 (2005) 250.
[30] N. Balasubramani, U.T.S. Pillai, B.C. Pai, Journal of Alloys and Compounds 457 (2008) 118.
[31] T.G. Nieh, J. Wadsworth, O.D. Sherby, Superplasticity in Metals and Ceramics, Cambridge University Press, Cambridge, 1997.
[32] R.Z. Valiev, Materials Science and Engineering A 59 (1997) 234.
[33] O.D. Sherby, J. Wadsworth, Progress in Materials Science 33 (1989) 169.
[34] X. Wu, Y. Liu, Scripta Materialia 46 (2002) 269.
[35] W.J. Kim, S.W. Chung, C.S. Chung, D. Kum, Acta Materialia 49 (2001) 3337.
[36] R.S. Chen, J.J. Blandin, M. Suery, Q.D. Wang, E.H. Han, Journal of Materials Science and Technology 20 (2004) 295.